



日本原子力研究開発機構機関リポジトリ  
Japan Atomic Energy Agency Institutional Repository

Title	Observation of $e^+e^- \rightarrow \pi^+\pi^-\pi^0 X_{b1,2}(1P)$ and search for $e^+e^- \rightarrow \phi X_{b1,2}(1P)$ at $\sqrt{s} = 10.96 - 11.05$ GeV
Author(s)	Yin J. H., Tanida Kiyoshi, Belle Collaboration, 189 of others
Citation	Physical Review D,98(9),p.091102_1-091102_9
Text Version	Published Journal Article
URL	<a href="https://jopss.jaea.go.jp/search/servlet/search?5065122">https://jopss.jaea.go.jp/search/servlet/search?5065122</a>
DOI	<a href="https://doi.org/10.1103/PhysRevD.98.091102">https://doi.org/10.1103/PhysRevD.98.091102</a>
Right	Published by the American Physical Society under the terms of the <a href="https://creativecommons.org/licenses/by/4.0/">Creative Commons Attribution 4.0 International</a> license. Further distribution of this work must maintain attribution to the author(s) and the published article's title, journal citation, and DOI. Funded by SCOAP3.



Japan Atomic Energy Agency

# **Observation of $e^+e^- \rightarrow \pi^+\pi^-\pi^0\chi_{b1,2}(1P)$ and search for $e^+e^- \rightarrow \phi\chi_{b1,2}(1P)$ at $\sqrt{s} = 10.96\text{--}11.05$ GeV**

J. H. Yin,<sup>27</sup> C. Z. Yuan,<sup>27</sup> I. Adachi,<sup>18,14</sup> H. Aihara,<sup>86</sup> S. Al Said,<sup>79,37</sup> D. M. Asner,<sup>4</sup> V. Aulchenko,<sup>5,66</sup> T. Aushev,<sup>55</sup> R. Ayad,<sup>79</sup> V. Babu,<sup>80</sup> I. Badhrees,<sup>79,36</sup> S. Bahinipati,<sup>22</sup> A. M. Bakich,<sup>78</sup> V. Bansal,<sup>68</sup> P. Behera,<sup>25</sup> C. Beleño,<sup>13</sup> B. Bhuyan,<sup>23</sup> T. Bilka,<sup>6</sup> J. Biswal,<sup>33</sup> A. Bobrov,<sup>5,66</sup> A. Bozek,<sup>63</sup> M. Bračko,<sup>49,33</sup> T. E. Browder,<sup>17</sup> L. Cao,<sup>34</sup> D. Červenkov,<sup>6</sup> P. Chang,<sup>62</sup> V. Chekelian,<sup>50</sup> A. Chen,<sup>60</sup> B. G. Cheon,<sup>16</sup> K. Chilikin,<sup>44</sup> K. Cho,<sup>38</sup> S.-K. Choi,<sup>15</sup> Y. Choi,<sup>77</sup> S. Choudhury,<sup>24</sup> D. Cinabro,<sup>90</sup> S. Cunliffe,<sup>9</sup> N. Dash,<sup>22</sup> S. Di Carlo,<sup>42</sup> J. Dingfelder,<sup>3</sup> Z. Doležal,<sup>6</sup> T. V. Dong,<sup>18,14</sup> Z. Drásal,<sup>6</sup> S. Eidelman,<sup>5,66,44</sup> D. Epifanov,<sup>5,66</sup> J. E. Fast,<sup>68</sup> T. Ferber,<sup>9</sup> B. G. Fulson,<sup>68</sup> R. Garg,<sup>69</sup> V. Gaur,<sup>89</sup> N. Gabyshev,<sup>5,66</sup> A. Garmash,<sup>5,66</sup> M. Gelb,<sup>34</sup> A. Giri,<sup>24</sup> P. Goldenzweig,<sup>34</sup> B. Golob,<sup>45,33</sup> J. Haba,<sup>18,14</sup> K. Hayasaka,<sup>65</sup> H. Hayashii,<sup>59</sup> S. Hirose,<sup>56</sup> W.-S. Hou,<sup>62</sup> T. Iijima,<sup>57,56</sup> K. Inami,<sup>56</sup> G. Inguglia,<sup>9</sup> A. Ishikawa,<sup>84</sup> R. Itoh,<sup>18,14</sup> M. Iwasaki,<sup>67</sup> Y. Iwasaki,<sup>18</sup> W. W. Jacobs,<sup>26</sup> I. Jaegle,<sup>10</sup> H. B. Jeon,<sup>41</sup> S. Jia,<sup>2</sup> Y. Jin,<sup>86</sup> D. Joffe,<sup>35</sup> K. K. Joo,<sup>7</sup> T. Julius,<sup>51</sup> K. H. Kang,<sup>41</sup> T. Kawasaki,<sup>65</sup> C. Kiesling,<sup>50</sup> D. Y. Kim,<sup>75</sup> J. B. Kim,<sup>39</sup> K. T. Kim,<sup>39</sup> S. H. Kim,<sup>16</sup> K. Kinoshita,<sup>8</sup> P. Kodyš,<sup>6</sup> S. Korpar,<sup>49,33</sup> D. Kotchetkov,<sup>17</sup> P. Križan,<sup>45,33</sup> R. Kroeger,<sup>52</sup> P. Krokovny,<sup>5,66</sup> T. Kuhr,<sup>46</sup> R. Kulasiri,<sup>35</sup> Y.-J. Kwon,<sup>92</sup> J. S. Lange,<sup>12</sup> I. S. Lee,<sup>16</sup> S. C. Lee,<sup>41</sup> L. K. Li,<sup>27</sup> Y. B. Li,<sup>70</sup> L. Li Gioi,<sup>50</sup> J. Libby,<sup>25</sup> D. Liventsev,<sup>89,18</sup> M. Lubej,<sup>33</sup> T. Luo,<sup>11</sup> M. Masuda,<sup>85</sup> T. Matsuda,<sup>53</sup> D. Matvienko,<sup>5,66,44</sup> M. Merola,<sup>30,58</sup> H. Miyata,<sup>65</sup> R. Mizuk,<sup>44,54,55</sup> G. B. Mohanty,<sup>80</sup> H. K. Moon,<sup>39</sup> T. Mori,<sup>56</sup> R. Mussa,<sup>31</sup> E. Nakano,<sup>67</sup> M. Nakao,<sup>18,14</sup> T. Nanut,<sup>33</sup> K. J. Nath,<sup>23</sup> Z. Natkaniec,<sup>63</sup> M. Nayak,<sup>90,18</sup> M. Niiyama,<sup>40</sup> N. K. Nisar,<sup>71</sup> S. Nishida,<sup>18,14</sup> K. Nishimura,<sup>17</sup> K. Ogawa,<sup>65</sup> S. Ogawa,<sup>83</sup> H. Ono,<sup>64,65</sup> P. Pakhlov,<sup>44,54</sup> G. Pakhlova,<sup>44,55</sup> B. Pal,<sup>4</sup> S. Pardi,<sup>30</sup> H. Park,<sup>41</sup> S. Paul,<sup>82</sup> T. K. Pedlar,<sup>47</sup> R. Pestotnik,<sup>33</sup> L. E. Piilonen,<sup>89</sup> V. Popov,<sup>44,55</sup> E. Prencipe,<sup>20</sup> A. Rostomyan,<sup>9</sup> G. Russo,<sup>30</sup> D. Sahoo,<sup>80</sup> Y. Sakai,<sup>18,14</sup> M. Salehi,<sup>48,46</sup> S. Sandilya,<sup>8</sup> L. Santelj,<sup>18</sup> T. Sanuki,<sup>84</sup> V. Savinov,<sup>71</sup> O. Schneider,<sup>43</sup> G. Schnell,<sup>1,21</sup> C. Schwanda,<sup>28</sup> Y. Seino,<sup>65</sup> K. Senyo,<sup>91</sup> O. Seon,<sup>56</sup> M. E. Sevier,<sup>51</sup> C. P. Shen,<sup>2</sup> T.-A. Shibata,<sup>87</sup> J.-G. Shiue,<sup>62</sup> B. Shwartz,<sup>5,66</sup> F. Simon,<sup>50,81</sup> A. Sokolov,<sup>29</sup> E. Solovieva,<sup>44,55</sup> M. Starič,<sup>33</sup> T. Sumiyoshi,<sup>88</sup> W. Sutcliffe,<sup>34</sup> M. Takizawa,<sup>74,19,72</sup> U. Tamponi,<sup>31</sup> K. Tanida,<sup>32</sup> F. Tenchini,<sup>51</sup> M. Uchida,<sup>87</sup> T. Uglov,<sup>44,55</sup> Y. Unno,<sup>16</sup> S. Uno,<sup>18,14</sup> P. Urquijo,<sup>51</sup> C. Van Hulse,<sup>1</sup> R. Van Tonder,<sup>34</sup> G. Varner,<sup>17</sup> A. Vinokurova,<sup>5,66</sup> V. Vorobyev,<sup>5,66,44</sup> B. Wang,<sup>8</sup> C. H. Wang,<sup>61</sup> M.-Z. Wang,<sup>62</sup> P. Wang,<sup>27</sup> X. L. Wang,<sup>11</sup> S. Watanuki,<sup>84</sup> E. Widmann,<sup>76</sup> E. Won,<sup>39</sup> H. Yamamoto,<sup>84</sup> H. Ye,<sup>9</sup> Y. Yusa,<sup>65</sup> Z. P. Zhang,<sup>73</sup> V. Zhilich,<sup>5,66</sup> V. Zhukova,<sup>44,54</sup> and V. Zhulanov,<sup>5,66</sup>

(Belle Collaboration)

<sup>1</sup>University of the Basque Country UPV/EHU, 48080 Bilbao

<sup>2</sup>Beihang University, Beijing 100191

<sup>3</sup>University of Bonn, 53115 Bonn

<sup>4</sup>Brookhaven National Laboratory, Upton, New York 11973

<sup>5</sup>Budker Institute of Nuclear Physics SB RAS, Novosibirsk 630090

<sup>6</sup>Faculty of Mathematics and Physics, Charles University, 121 16 Prague

<sup>7</sup>Chonnam National University, Kwangju 660-701

<sup>8</sup>University of Cincinnati, Cincinnati, Ohio 45221

<sup>9</sup>Deutsches Elektronen-Synchrotron, 22607 Hamburg

<sup>10</sup>University of Florida, Gainesville, Florida 32611

<sup>11</sup>Key Laboratory of Nuclear Physics and Ion-beam Application (MOE) and Institute of Modern Physics, Fudan University, Shanghai 200443

<sup>12</sup>Justus-Liebig-Universität Gießen, 35392 Gießen

<sup>13</sup>II. Physikalisches Institut, Georg-August-Universität Göttingen, 37073 Göttingen

<sup>14</sup>SOKENDAI (The Graduate University for Advanced Studies), Hayama 240-0193

<sup>15</sup>Gyeongsang National University, Chinju 660-701

<sup>16</sup>Hanyang University, Seoul 133-791

<sup>17</sup>University of Hawaii, Honolulu, Hawaii 96822

<sup>18</sup>High Energy Accelerator Research Organization (KEK), Tsukuba 305-0801

<sup>19</sup>J-PARC Branch, KEK Theory Center, High Energy Accelerator Research Organization (KEK), Tsukuba 305-0801

<sup>20</sup>Forschungszentrum Jülich, 52425 Jülich

<sup>21</sup>IKERBASQUE, Basque Foundation for Science, 48013 Bilbao

<sup>22</sup>Indian Institute of Technology Bhubaneswar, Satya Nagar 751007

<sup>23</sup>Indian Institute of Technology Guwahati, Assam 781039

<sup>24</sup>Indian Institute of Technology Hyderabad, Telangana 502285

- <sup>25</sup>Indian Institute of Technology Madras, Chennai 600036
- <sup>26</sup>Indiana University, Bloomington, Indiana 47408
- <sup>27</sup>Institute of High Energy Physics, Chinese Academy of Sciences, Beijing 100049
- <sup>28</sup>Institute of High Energy Physics, Vienna 1050
- <sup>29</sup>Institute for High Energy Physics, Protvino 142281
- <sup>30</sup>INFN—Sezione di Napoli, 80126 Napoli
- <sup>31</sup>INFN—Sezione di Torino, 10125 Torino
- <sup>32</sup>Advanced Science Research Center, Japan Atomic Energy Agency, Naka 319-1195
- <sup>33</sup>J. Stefan Institute, 1000 Ljubljana
- <sup>34</sup>Institut für Experimentelle Teilchenphysik, Karlsruher Institut für Technologie, 76131 Karlsruhe
- <sup>35</sup>Kennesaw State University, Kennesaw, Georgia 30144
- <sup>36</sup>King Abdulaziz City for Science and Technology, Riyadh 11442
- <sup>37</sup>Department of Physics, Faculty of Science, King Abdulaziz University, Jeddah 21589
- <sup>38</sup>Korea Institute of Science and Technology Information, Daejeon 305-806
- <sup>39</sup>Korea University, Seoul 136-713
- <sup>40</sup>Kyoto University, Kyoto 606-8502
- <sup>41</sup>Kyungpook National University, Daegu 702-701
- <sup>42</sup>LAL, Université Paris-Sud, CNRS/IN2P3, Université Paris-Saclay, Orsay
- <sup>43</sup>École Polytechnique Fédérale de Lausanne (EPFL), Lausanne 1015
- <sup>44</sup>P.N. Lebedev Physical Institute of the Russian Academy of Sciences, Moscow 119991
- <sup>45</sup>Faculty of Mathematics and Physics, University of Ljubljana, 1000 Ljubljana
- <sup>46</sup>Ludwig Maximilians University, 80539 Munich
- <sup>47</sup>Luther College, Decorah, Iowa 52101
- <sup>48</sup>University of Malaya, 50603 Kuala Lumpur
- <sup>49</sup>University of Maribor, 2000 Maribor
- <sup>50</sup>Max-Planck-Institut für Physik, 80805 München
- <sup>51</sup>School of Physics, University of Melbourne, Victoria 3010
- <sup>52</sup>University of Mississippi, University, Mississippi 38677
- <sup>53</sup>University of Miyazaki, Miyazaki 889-2192
- <sup>54</sup>Moscow Physical Engineering Institute, Moscow 115409
- <sup>55</sup>Moscow Institute of Physics and Technology, Moscow Region 141700
- <sup>56</sup>Graduate School of Science, Nagoya University, Nagoya 464-8602
- <sup>57</sup>Kobayashi-Maskawa Institute, Nagoya University, Nagoya 464-8602
- <sup>58</sup>Università di Napoli Federico II, 80055 Napoli
- <sup>59</sup>Nara Women's University, Nara 630-8506
- <sup>60</sup>National Central University, Chung-li 32054
- <sup>61</sup>National United University, Miao Li 36003
- <sup>62</sup>Department of Physics, National Taiwan University, Taipei 10617
- <sup>63</sup>H. Niewodniczanski Institute of Nuclear Physics, Krakow 31-342
- <sup>64</sup>Nippon Dental University, Niigata 951-8580
- <sup>65</sup>Niigata University, Niigata 950-2181
- <sup>66</sup>Novosibirsk State University, Novosibirsk 630090
- <sup>67</sup>Osaka City University, Osaka 558-8585
- <sup>68</sup>Pacific Northwest National Laboratory, Richland, Washington 99352
- <sup>69</sup>Panjab University, Chandigarh 160014
- <sup>70</sup>Peking University, Beijing 100871
- <sup>71</sup>University of Pittsburgh, Pittsburgh, Pennsylvania 15260
- <sup>72</sup>Theoretical Research Division, Nishina Center, RIKEN, Saitama 351-0198
- <sup>73</sup>University of Science and Technology of China, Hefei 230026
- <sup>74</sup>Showa Pharmaceutical University, Tokyo 194-8543
- <sup>75</sup>Soongsil University, Seoul 156-743
- <sup>76</sup>Stefan Meyer Institute for Subatomic Physics, Vienna 1090
- <sup>77</sup>Sungkyunkwan University, Suwon 440-746
- <sup>78</sup>School of Physics, University of Sydney, New South Wales 2006
- <sup>79</sup>Department of Physics, Faculty of Science, University of Tabuk, Tabuk 71451
- <sup>80</sup>Tata Institute of Fundamental Research, Mumbai 400005
- <sup>81</sup>Excellence Cluster Universe, Technische Universität München, 85748 Garching
- <sup>82</sup>Department of Physics, Technische Universität München, 85748 Garching
- <sup>83</sup>Toho University, Funabashi 274-8510
- <sup>84</sup>Department of Physics, Tohoku University, Sendai 980-8578

<sup>85</sup>*Earthquake Research Institute, University of Tokyo, Tokyo 113-0032*<sup>86</sup>*Department of Physics, University of Tokyo, Tokyo 113-0033*<sup>87</sup>*Tokyo Institute of Technology, Tokyo 152-8550*<sup>88</sup>*Tokyo Metropolitan University, Tokyo 192-0397*<sup>89</sup>*Virginia Polytechnic Institute and State University, Blacksburg, Virginia 24061*<sup>90</sup>*Wayne State University, Detroit, Michigan 48202*<sup>91</sup>*Yamagata University, Yamagata 990-8560*<sup>92</sup>*Yonsei University, Seoul 120-749*

(Received 18 June 2018; published 15 November 2018)

We report searches for the processes  $e^+e^- \rightarrow \pi^+\pi^-\pi^0\chi_{bJ}$  and  $e^+e^- \rightarrow \phi\chi_{bJ}$  ( $J = 1, 2$ ) based on data samples collected by the Belle experiment at the KEKB collider. We report the first observation of the process  $e^+e^- \rightarrow (\pi^+\pi^-\pi^0)_{\text{non-}\omega}\chi_{b1}$  and first evidence for  $e^+e^- \rightarrow \omega\chi_{bJ}$  in the vicinity of the  $\Upsilon(11020)$  resonance, with center-of-mass energies from 10.96 to 11.05 GeV. The significances for  $(\pi^+\pi^-\pi^0)_{\text{non-}\omega}\chi_{b1}$  and  $\omega\chi_{bJ}$  are greater than  $5.3\sigma$  and  $4.0\sigma$ , respectively. We also investigate the energy dependence of the  $e^+e^- \rightarrow \pi^+\pi^-\pi^0\chi_{bJ}$  cross section, but we cannot determine whether the contributions are from the  $\Upsilon(10860)$  and  $\Upsilon(11020)$  resonances or nonresonant continuum processes. The signals for  $e^+e^- \rightarrow \phi\chi_{bJ}$  are not significant, and the upper limits of the Born cross sections at the 90% confidence level are 0.7 and 1.0 pb for  $e^+e^- \rightarrow \phi\chi_{b1}$  and  $\phi\chi_{b2}$ , respectively, for center-of-mass energies from 10.96 to 11.05 GeV.

DOI: [10.1103/PhysRevD.98.091102](https://doi.org/10.1103/PhysRevD.98.091102)

Hadronic transitions among heavy quarkonium states serve as a key source of information for better understanding the strong interaction between a quark and antiquark, and thus quantum chromodynamics (QCD). The heavy quarkonium systems, in which the speed of quarks is sufficiently small, are approximately nonrelativistic, and the hadronic transitions to lower lying states have long been described using the QCD multipole expansion [1]. However, the existence of anomalously large hadronic transition rates from the  $\Upsilon(10860)$ , as reported by the Belle experiment [2–9], challenges the theoretical calculations, as well as the pure bottomonium nature of the  $\Upsilon(10860)$  and  $\Upsilon(11020)$  [10–12].

The processes  $e^+e^- \rightarrow \omega\chi_{bJ}$  were observed recently [4] using data samples taken at energies near the  $\Upsilon(10860)$  peak, but the dependence of the  $e^+e^- \rightarrow \omega\chi_{bJ}$  cross section versus energy was not measured. Therefore, it is unclear whether this process occurs from the  $\Upsilon(10860)$  meson or continuum process. Nevertheless, the result has been investigated extensively by theorists to understand the dynamics of these transitions, producing studies of  $S$ - and  $D$ -wave mixing for the observed heavy quark spin-symmetry violation from the comparison of  $\omega\chi_{b1}$  and  $\omega\chi_{b2}$  [13], a possible contribution of  $\Upsilon(10860) \rightarrow \pi Z_b \rightarrow \pi\rho\Upsilon(1S)$  [14], a molecular component in the  $\Upsilon(10860)$  wave function [14], and hadronic-loop effects [15].

By extending the calculation in Ref. [15] to the  $\Upsilon(11020)$  case, assuming the hadronic-loop effect is a universal mechanism in the higher bottomonium transitions, the authors of Ref. [16] predict the branching fractions of  $\Upsilon(11020) \rightarrow \omega\chi_{bJ}$  in addition to  $\Upsilon(11020) \rightarrow \phi\chi_{bJ}$ , where  $J = 0, 1$ , and  $2$ , as listed in Table I. Relative magnitudes of these branching fractions are also predicted (and listed in Table I), which are weakly dependent on the free parameters introduced in the theoretical calculation. An experimental measurement of these  $\omega$  and  $\phi$  transitions will give a crucial test on how well the hadronic-loop effect works in  $\Upsilon(11020)$  decay, and a test of the similarity between  $\Upsilon(11020)$  and  $\Upsilon(10860)$ .

In this paper, we report the results of a search for  $\omega\chi_{bJ}$  and  $\phi\chi_{bJ}$  using the  $\Upsilon(10860)$  and  $\Upsilon(11020)$  energy scan data collected with the Belle detector. The data that we are using consist of 22 samples of high integrated luminosity (listed in Table II), and 18 additional samples of about  $50 \text{ pb}^{-1}$  per point taken in 5 MeV steps between 10.96 and 11.05 GeV [17]. We use  $\chi_{bJ} \rightarrow \gamma\Upsilon(1S)$ ,  $\Upsilon(1S) \rightarrow \ell^+\ell^-$  ( $\ell = e, \mu$ ),  $\omega \rightarrow \pi^+\pi^-\pi^0$  to reconstruct the  $e^+e^- \rightarrow \omega\chi_{b1,2}$  signal; for the  $e^+e^- \rightarrow \phi\chi_{bJ}$  signal, we reconstruct  $\phi$  with its decays to  $K^+K^-$  and check the production of  $\chi_{bJ}$  by studying the  $K^+K^-$  recoil mass.

The Belle detector, located at the KEKB asymmetric-energy  $e^+e^-$  collider [18] is described in Ref. [19]. The EVTGEN [20] generator, as well as a GEANT3 [21]-based detector simulation, is used to produce simulated events using Monte Carlo (MC) methods. The nominal parameters of the states in the decay chains are quoted from Ref. [22]. To take the initial-state radiation (ISR) into consideration, the radiator function from Ref. [23] is introduced in EVTGEN. A generic MC sample at the  $\Upsilon(10860)$  peak

TABLE I. The predicted branching fractions of  $\Upsilon(11020) \rightarrow \omega\chi_{bJ}$  and  $\phi\chi_{bJ}$  [16], as well as the relative magnitudes, where  $\mathcal{B}_j \equiv \mathcal{B}(\Upsilon(11020) \rightarrow \omega(\phi)\chi_{bJ})$ ,  $R_{ij} \equiv \frac{\mathcal{B}_i}{\mathcal{B}_j}$ .

Decay mode	$\mathcal{B}_0$	$\mathcal{B}_1$	$\mathcal{B}_2$	$R_{10}$	$R_{20}$	$R_{21}$
$\omega\chi_{bJ}$	$(0.15\text{--}2.81) \times 10^{-3}$	$(0.63\text{--}11.68) \times 10^{-3}$	$(1.08\text{--}20.02) \times 10^{-3}$	$\approx 4.11$	$\approx 7.06$	$\approx 1.72$
$\phi\chi_{bJ}$	$(0.68\text{--}4.62) \times 10^{-6}$	$(0.50\text{--}3.43) \times 10^{-6}$	$(2.22\text{--}15.18) \times 10^{-6}$	$\approx 0.74$	$\approx 3.28$	$\approx 4.43$

including all possible decays is used to study the possible background channels and investigate the background shape.

For charged tracks, the impact parameters perpendicular to and along the beam direction with respect to the interaction point are required to be less than 1.0 and 3.5 cm, respectively. The transverse momentum is restricted to be higher than 0.1 GeV/ $c$ . A particle identification (PID) hypothesis  $\mathcal{L}(X)$  for each charged track is formed from different detector subsystems for particle  $X \in e, \mu, \pi, K, p$ . Tracks with a likelihood ratio  $\mathcal{R}(K) = \mathcal{L}(K)/(\mathcal{L}(K) + \mathcal{L}(\pi)) < 0.4$  are identified as pions while those with  $\mathcal{R}(K) > 0.6$  are identified as kaons. Similarly, we define the likelihood ratios  $\mathcal{R}(e)$  and  $\mathcal{R}(\mu)$  for identification of electrons and muons, respectively, with  $\mathcal{R}(e) > 0.01$  and  $\mathcal{R}(\mu) > 0.1$ . A neutral cluster in the electromagnetic calorimeter is reconstructed as a photon

TABLE II. Integrated luminosity at different c.m. energy as well as the energy-dependent Born cross sections for  $e^+e^- \rightarrow \pi^+\pi^-\pi^0\chi_{bJ}$  with statistical uncertainty only. A 11.9% common systematic uncertainty is not included.

$E_{\text{c.m.}}$ (GeV)	$\mathcal{L}$ (fb $^{-1}$ )	$\sigma^{\text{Born}}(\pi^+\pi^-\pi^0\chi_{bJ})$ (pb)
10.7711	0.955	$-1.44^{+2.62}_{-1.74}$
10.8203	1.164	$2.72^{+2.07}_{-1.43}$
10.8497	0.989	$2.70^{+2.19}_{-1.41}$
10.8589	0.989	$0.64^{+1.51}_{-0.75}$
10.8633	47.648	$0.82^{+0.10}_{-0.10}$
10.8667	45.553	$0.68^{+0.10}_{-0.10}$
10.8686	22.938	$0.89^{+0.16}_{-0.16}$
10.8695	0.978	$1.23^{+1.96}_{-1.21}$
10.8785	0.978	$1.90^{+1.90}_{-1.17}$
10.8836	1.230	$1.37^{+1.56}_{-1.01}$
10.8889	0.989	$1.20^{+1.63}_{-0.93}$
10.8985	0.983	$1.14^{+1.55}_{-0.88}$
10.9011	0.873	$-1.25^{+1.82}_{-1.06}$
10.9077	0.980	$0.51^{+1.50}_{-0.87}$
10.9275	0.667	$2.12^{+2.11}_{-1.30}$
10.9575	0.851	$0.70^{+1.67}_{-0.83}$
10.9775	0.999	$2.84^{+1.96}_{-1.32}$
10.9919	0.986	$1.10^{+1.50}_{-0.87}$
11.0068	0.976	$3.05^{+1.86}_{-1.28}$
11.0164	0.771	$3.47^{+2.11}_{-1.46}$
11.0175	0.849	$0.00^{+0.95}_{-0.32}$
11.0220	0.982	$0.84^{+1.49}_{-0.98}$

if it does not match the extrapolated position of any charged track and its energy is greater than 30 MeV.

To select  $e^+e^- \rightarrow \pi^+\pi^-\pi^0\chi_{bJ}$  candidates, we require that there be exactly four tracks with zero net charge, of which two are positively identified as pions and the other two as leptons. At least three photons are required in the event, and a  $\pi^0$  list is created with the invariant mass of the photon pairs satisfying  $M(\gamma\gamma) \in [0.12, 0.15]$  GeV/ $c^2$ , which covers nearly  $\pm 3\sigma$  around the  $\pi^0$  peak. To improve the track momentum and photon energy resolutions, and to suppress the background, a five-constraint (5C) kinematic fit is performed for the  $\gamma\pi^+\pi^-\pi^0\ell^+\ell^-$  candidates enforcing energy and momentum conservation and constraining the invariant mass of  $\pi^0$  candidates. The four momenta of the final-state particles after the 5C kinematic fit are kept for further analysis. The  $\chi^2_{5C}/\text{ndf}$  is required to be less than 20, where  $\chi^2_{5C}$  is the resulting  $\chi^2$  of the kinematic fit, and  $\text{ndf} = 5$  is the number of degrees of freedom. If there are multiple  $\pi^0$  candidates surviving the kinematic fit in an event, the one with the smallest  $\chi^2_{5C}$  is kept. The lepton pair is taken as an  $\Upsilon(1S)$  candidate if its invariant mass is in the region  $[9.42, 9.60]$  GeV/ $c^2$ .

The  $\chi_{bJ}$  candidates are reconstructed with the selected  $\Upsilon(1S)$  and the photon not used to form a  $\pi^0$  candidate. The invariant mass of  $\pi^+\pi^-\pi^0$  ( $M(\pi^+\pi^-\pi^0)$ ) versus the corrected invariant mass of  $\gamma\Upsilon(1S)$  ( $M(\gamma\Upsilon(1S)) \equiv M(\gamma\ell^+\ell^-) - M(\ell^+\ell^-) + m_{\Upsilon(1S)}$ ) is shown in Fig. 1 for the sum of the data samples in the  $\Upsilon(11020)$  energy region, which is defined as  $E_{\text{c.m.}} > 10.96$  GeV. Clusters of events for the production of  $\chi_{bJ}$  can be seen both when  $M(\pi^+\pi^-\pi^0)$  is in the  $\omega$  mass region ( $[0.75, 0.81]$  GeV/ $c^2$ ) and at higher masses ( $> 0.81$  GeV/ $c^2$ ). For events having  $M(\pi^+\pi^-\pi^0)$  in the  $\omega$  mass region, the  $\chi_{b2}$  signal is dominant while for signal events with higher  $\pi^+\pi^-\pi^0$  masses, the  $\chi_{b1}$  signal is dominant. The background in this case comes predominantly from false  $\pi^0$  candidates produced by combinatorial photons.

An unbinned two-dimensional (2D) extended maximum likelihood fit to the  $M(\pi^+\pi^-\pi^0)$  and  $M(\gamma\Upsilon(1S))$  distributions of the candidate events is applied to determine the numbers of  $\omega\chi_{bJ}$  and  $\pi^+\pi^-\pi^0\chi_{bJ}$  events. In the fit, the shapes of  $\omega\chi_{bJ}$  and  $\pi^+\pi^-\pi^0\chi_{bJ}$  obtained from MC simulation are used to describe the signals, and a 2D function  $f(x, y) = ax + by$  ( $x = M(\gamma\Upsilon(1S))$  and  $y = M(\pi^+\pi^-\pi^0)$ ) is used to fit the background. Here the  $\pi^+\pi^-\pi^0\chi_{bJ}$  MC sample is generated following a four-body phase space



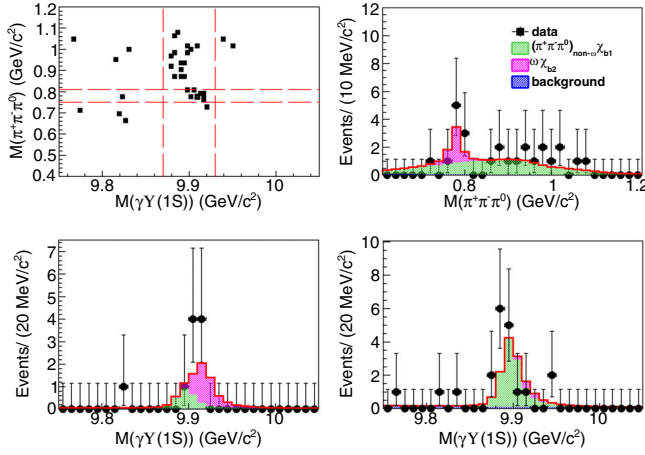


FIG. 1. A scatter plot of  $M(\pi^+\pi^-\pi^0)$  versus  $M(\gamma\Upsilon(1S))$  from data (top left), and the projections of the 2D fit for events in the  $\chi_{bJ}$  signal region (top right), in the  $\omega$  signal region (bottom left), and out of the  $\omega$  signal region (bottom right).

(PHSP) distribution, and this process is denoted as  $(\pi^+\pi^-\pi^0)_{\text{non-}\omega}\chi_{bJ}$ . The projections of the fit results for events in the  $\chi_{bJ}$  signal region ( $M(\gamma\Upsilon(1S)) \in [9.87, 9.93]$  GeV/c²), in the  $\omega$  signal region, and in the region above the  $\omega$  mass are also shown in Fig. 1. The statistical significances for  $(\pi^+\pi^-\pi^0)_{\text{non-}\omega}\chi_{b1}$ ,  $(\pi^+\pi^-\pi^0)_{\text{non-}\omega}\chi_{b2}$ ,  $\omega\chi_{b1}$  and  $\omega\chi_{b2}$  are  $5.3\sigma$ ,  $0.0\sigma$ ,  $0.0\sigma$  and  $2.5\sigma$ , respectively. The significances are calculated based on the change in likelihood when the signal yield is set to zero in the fit [25]. The signal yields for  $(\pi^+\pi^-\pi^0)_{\text{non-}\omega}\chi_{b1}$  and  $\omega\chi_{b2}$  are  $19.6 \pm 5.3$  and  $7.8 \pm 3.2$ , respectively, and the signal yields for  $\omega\chi_{b1}$  and  $(\pi^+\pi^-\pi^0)_{\text{non-}\omega}\chi_{b2}$  are consistent with zero. Then we assume that either the processes  $(\pi^+\pi^-\pi^0)_{\text{non-}\omega}\chi_{b1}$  and  $(\pi^+\pi^-\pi^0)_{\text{non-}\omega}\chi_{b2}$  exist at the same time, or the processes  $\omega\chi_{b1}$  and  $\omega\chi_{b2}$  exist at the same time, and the fit is repeated. The statistical significances for  $(\pi^+\pi^-\pi^0)_{\text{non-}\omega}\chi_{bJ}$  and  $\omega\chi_{bJ}$  are  $6.1\sigma$  and  $4.0\sigma$ , respectively. The changes on the significances arise from the similarity in signal shapes between  $(\pi^+\pi^-\pi^0)_{\text{non-}\omega}\chi_{b1}$  and  $(\pi^+\pi^-\pi^0)_{\text{non-}\omega}\chi_{b2}$ , and between  $\omega\chi_{b1}$  and  $\omega\chi_{b2}$ . Thus, evidence for  $\omega\chi_{bJ}$  has been found, but we cannot determine whether the events are from  $\omega\chi_{b1}$  or  $\omega\chi_{b2}$ . We also use other forms of background descriptions as systematics. Changes in the signal yields and significances are negligible.

In order to study the energy dependent cross section of  $\pi^+\pi^-\pi^0\chi_{b1}$  and  $\pi^+\pi^-\pi^0\chi_{b2}$  events, we extract the observed signal yields  $N_{\text{obs}}$  with data samples listed in Table II. Because of the limited statistics for most energy points, we do not perform a 2D fit as for the summed sample, nor do we separate  $\pi^+\pi^-\pi^0$  into  $\omega$  and non- $\omega$ , nor  $\gamma\Upsilon(1S)$  into  $\chi_{b1}$  and  $\chi_{b2}$ . The number of  $\chi_{bJ}$  signal events in each sample is computed using the formula:  $N_{\text{obs}} = N_{\text{sig}} - N_{\text{side}}$ , where  $N_{\text{sig}}$  is the number of events in the  $\chi_{bJ}$  signal region and  $N_{\text{side}}$  is that in the sideband region. Here the signal region is

defined as  $M(\gamma\Upsilon(1S)) \in [9.852, 9.952]$  GeV/c², while the sideband region is  $[9.77, 9.82]$  and  $[9.98, 10.03]$  GeV/c².

The Born cross sections are calculated with

$$\sigma^{\text{Born}} = \frac{N_{\text{obs}}}{\epsilon \mathcal{B}_{\text{inter}} \mathcal{L} (1 + \delta) / |1 - \Pi|^2}, \quad (1)$$

where  $\epsilon$  is the reconstructed efficiency,  $\mathcal{B}_{\text{inter}}$  is the corresponding product of intermediate decay branching fractions,  $\mathcal{L}$  is the integrated luminosity,  $(1 + \delta)$  is the ISR correction factor, and  $(1/|1 - \Pi|^2)$  is the vacuum polarization factor [26]. We use the weighted branching fraction  $\mathcal{B}_{\text{inter}} = \mathcal{B}(\chi_{b1} \rightarrow \gamma\Upsilon(1S)) \cdot f + \mathcal{B}(\chi_{b2} \rightarrow \gamma\Upsilon(1S)) \cdot (1 - f)$ , where  $f = N_1 / (N_1 + N_2) = 0.74 \pm 0.06$  is the fraction of  $\chi_{b1}$  in the process  $e^+e^- \rightarrow \pi^+\pi^-\pi^0\chi_{bJ}$  near the  $\Upsilon(10860)$  peak [4]. In order to estimate the ISR correction factors, we use

$$1 + \delta = \frac{\int_0^{1 - \frac{m_0^2}{s}} G_{\text{BW}}(s(1 - x)) F(x, s) dx}{G_{\text{BW}}(s)}, \quad (2)$$

where  $m_0$  is the mass threshold of  $\pi^+\pi^-\pi^0\chi_{bJ}$ ,  $F(x, s)$  is the radiative function [23] and  $G_{\text{BW}}(s)$  is the Breit-Wigner (BW) function,

$$G_{\text{BW}}(s) = \frac{12\pi\Gamma_{ee} \cdot \mathcal{B} \cdot \Gamma_{\text{tot}}}{(s - M^2)^2 + M^2\Gamma_{\text{tot}}^2} \times \frac{\Phi(s)}{\Phi(M)}, \quad (3)$$

where  $M$  is the nominal mass of  $\Upsilon(10860)$  or  $\Upsilon(11020)$ ,  $\Gamma_{\text{tot}}$  is the total width,  $\Gamma_{ee}$  is the partial decay width of  $e^+e^-$  channel,  $\mathcal{B}$  is the branching fractions of  $\pi^+\pi^-\pi^0\chi_{bJ}$ , and  $\Phi$  is given by considering  $\pi^+\pi^-\pi^0$  as a wide resonance with mass distribution generated in four-body  $e^+e^- \rightarrow \pi^+\pi^-\pi^0\chi_{bJ}$  phase space.

The energy-dependent cross sections for  $e^+e^- \rightarrow \pi^+\pi^-\pi^0\chi_{bJ}$  are listed in Table II and plotted in Fig. 2. A maximum likelihood fit of the cross sections is performed.

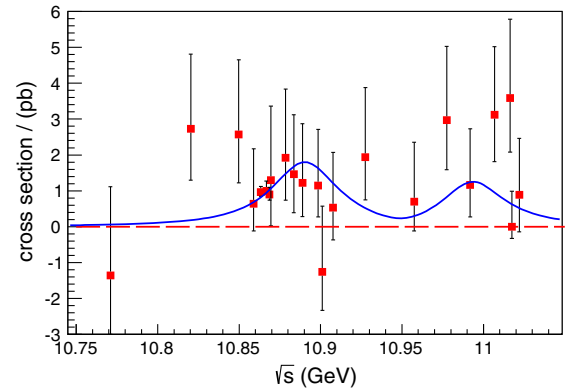


FIG. 2. Fit to the cross sections of  $e^+e^- \rightarrow \pi^+\pi^-\pi^0\chi_{bJ}$  as described in the text. The red boxes with error bars are the cross sections of  $e^+e^- \rightarrow \pi^+\pi^-\pi^0\chi_{bJ}$  and the solid blue curve is the fit.

The likelihood for the three data samples of larger integrated luminosity around 10.865 GeV is calculated assuming the number of signal events follows the Gaussian distribution:

$$L(\mu_{\text{sig}}; N_{\text{obs}}, \sigma) = \frac{1}{\sqrt{2\pi}\sigma'} e^{-\frac{(\mu_{\text{sig}} - N_{\text{obs}})^2}{2\sigma'^2}}, \quad (4)$$

where  $\mu_{\text{sig}}$  is the number of expected signal events, and  $\sigma'$  is the statistical uncertainty of  $N_{\text{obs}}$ . For the other samples, the likelihood is calculated assuming the number of signal events follows the Poisson distribution:

$$L(\mu_{\text{sig}}; N_{\text{sig}}, N_{\text{side}}) = \int_0^\infty P(N_{\text{sig}}; \mu_{\text{sig}} + \mu_{\text{bkg}}) P(N_{\text{side}}; \mu_{\text{bkg}}) d\mu_{\text{bkg}}, \quad (5)$$

where  $P(N; \mu) = \frac{1}{N!} \mu^N e^{-\mu}$  is the probability density function of the Poisson distribution, and  $\mu_{\text{bkg}}$  is the number of expected background events. Since the known cross section energy dependences, i.e., those of  $\pi\pi\Upsilon(nS)$  [8] and  $\pi\pi h_b(mP)$  [9], exhibit  $\Upsilon(10860)$  and  $\Upsilon(11020)$  peaks but no nonresonant contributions. The fit function here is also a coherent sum of two BW amplitudes in the form of Eq. (3) for  $\Upsilon(10860)$  and  $\Upsilon(11020)$ , and the masses and widths are fixed to their world average values [22] while the corresponding products  $\Gamma_{ee} \cdot \mathcal{B}$  are left free. The fit results are shown in Fig. 2. Two solutions are found that differ in phase, but the resulting  $\Gamma_{ee} \cdot \mathcal{B}$  are consistent with each other. The obtained product branching fractions are  $\mathcal{B}(\Upsilon(10860) \rightarrow e^+e^-) \cdot \mathcal{B}(\Upsilon(10860) \rightarrow \pi^+\pi^-\pi^0\chi_{bJ}) = (15.3 \pm 3.7) \times 10^{-9}$ ,  $\mathcal{B}(\Upsilon(11020) \rightarrow e^+e^-) \cdot \mathcal{B}(\Upsilon(11020) \rightarrow \pi^+\pi^-\pi^0\chi_{bJ}) = (18.3 \pm 9.0) \times 10^{-9}$ , where the errors are statistical. We also try to introduce a coherent continuum component into the fit, but the significance of this hypothesis is only  $1.4\sigma$ . The introduction of the continuum term results in a change of the  $\Upsilon(10860)$  product branching fraction of  $12.6 \times 10^{-9}$  and that of the  $\Upsilon(11020)$  product branching fraction of  $12.8 \times 10^{-9}$ , which are taken as systematic uncertainty due to “continuum contribution.”

There are several sources of systematic error in the cross section measurements, and most of the uncertainties are similar to the previous work [4], including tracking efficiency (1.0% per pion and kaon track and 0.35% per lepton), PID efficiency (1.3% per pion and 1.6% per lepton), photon energy resolution calibration (1.1%),  $\pi^0$  selection (2.2%), 5C kinematic fit (4.2%), and trigger simulation (3.0%). The uncertainty from luminosity is 1.5% [9]. Comparing the reconstruction efficiency with the ISR process in EVTGEN with the efficiency without the ISR process added to EVTGEN, but still corrected for with the ISR correction factor, yields an uncertainty of 1.0%. The corresponding uncertainty from the branching fractions of  $\chi_{bJ} \rightarrow \gamma\Upsilon(1S)$ ,  $\Upsilon(1S) \rightarrow \ell^+\ell^-$  is 8.2% [22].

The total systematic uncertainty, 11.9%, is obtained by adding all the above results in quadrature.

The systematic uncertainty in the measured branching fractions rises from the cross section measurements and the fit to those cross sections. The systematic uncertainties in the fit to the cross sections mainly come from the parametrization of the BW function, PHSP factor, resonance parameters, and the possible continuum contribution. The first is estimated by replacing the constant width with an energy dependent width  $\Gamma_{\text{tot}} = \Gamma_{\text{tot}}^0 \cdot \Phi(\sqrt{s})/\Phi(M)$ . The second source is estimated by replacing the PHSP factor of  $\pi^+\pi^-\pi^0\chi_{bJ}$  with the two-body PHSP factor of  $\omega\chi_{bJ}$ . The third source is estimated by varying the resonance parameters  $\Upsilon(10860)$  and  $\Upsilon(11020)$  within  $\pm 1\sigma$ . The final systematic uncertainty is estimated by adding a coherent continuum contribution to the fit function. The changes of the branching fractions are taken as the symmetrized systematic uncertainty. The details are listed in Table III.

By using  $\mathcal{B}(\Upsilon(10860) \rightarrow e^+e^-) = (6.1 \pm 1.6) \times 10^{-6}$  and  $\mathcal{B}(\Upsilon(11020) \rightarrow e^+e^-) = (2.1_{-0.6}^{+1.1}) \times 10^{-6}$  [22], we obtain  $\mathcal{B}(\Upsilon(10860) \rightarrow \pi^+\pi^-\pi^0\chi_{bJ}) = (2.5 \pm 0.6 \pm 2.1 \pm 0.7) \times 10^{-3}$ ,  $\mathcal{B}(\Upsilon(11020) \rightarrow \pi^+\pi^-\pi^0\chi_{bJ}) = (8.7 \pm 4.3 \pm 6.1_{-2.5}^{+4.5}) \times 10^{-3}$ , where the first errors are statistical, the second are systematic errors combined from the cross section measurements and line shape fit, and the third result from the branching fractions of  $\Upsilon(10860)$  and  $\Upsilon(11020) \rightarrow e^+e^-$  [22].

To reconstruct  $e^+e^- \rightarrow \phi\chi_{bJ}$ , we require at least two kaons in one event. There is no requirement on the number of photons, but a list of photon candidates is created in one event satisfying  $|M(\gamma\gamma_2) - m_{\pi^0}| > 13 \text{ MeV}/c^2$ , where  $\gamma_2$  is any other photon in the event with  $E_{\gamma_2} > 0.1 \text{ GeV}$ , and  $m_{\pi^0}$  is the nominal mass of the  $\pi^0$ . The data are divided into two categories. One includes events when one of the photons in the above list satisfies  $M(\gamma K^+ K^-)_{\text{recoil}} \equiv \sqrt{(\sqrt{s} - E_{\gamma K^+ K^-})^2 - (\vec{p}_{\gamma K^+ K^-})^2} \in [9.42, 9.50] \text{ GeV}/c^2$ , i.e., in the  $\Upsilon(1S)$  mass region, to tag  $\chi_{bJ} \rightarrow \gamma\Upsilon(1S)$  events; the other includes all other events, to tag  $\chi_{bJ} \rightarrow \text{non} - \gamma\Upsilon(1S)$  events. Here  $(\vec{p}_{\gamma K^+ K^-}, E_{\gamma K^+ K^-})$  is the four momenta of  $\gamma K^+ K^-$  system in c.m. frame.

TABLE III. Summary of the absolute systematic uncertainties in product branching fractions ( $\times 10^{-9}$ ), where  $\mathcal{B}(10860, 11020)$  represent  $\mathcal{B}(\Upsilon(10860, 11020) \rightarrow e^+e^-) \cdot \mathcal{B}(\Upsilon(10860, 11020) \rightarrow \pi^+\pi^-\pi^0\chi_{bJ})$ .

$\pi^+\pi^-\pi^0\chi_{bJ}$	$\mathcal{B}(10860)$	$\mathcal{B}(11020)$
Cross sections	1.8	2.1
BW parametrization	0.6	0.4
PHSP factor	0.6	0.2
Resonance parameters	2.4	1.6
Continuum contribution	12.2	12.6
Sum	12.6	12.8

We use the figure of merit,  $\mathcal{S}/\sqrt{\mathcal{S}+\mathcal{B}}$ , to optimize the  $K^+K^-$  invariant mass window requirement. Here  $\mathcal{S}$  is the reconstructed number of signal events obtained from MC simulation of the signal process,  $\Upsilon(11020) \rightarrow \phi\chi_{bJ}$  with  $\phi \rightarrow K^+K^-$ ,  $\chi_{bJ} \rightarrow \text{anything}$ , in the signal region,  $[9.88, 9.93] \text{ GeV}/c^2$ . The number is normalized according to the theoretical calculation of the branching fraction of  $\Upsilon(11020) \rightarrow \phi\chi_{bJ}$  [16] and the total  $\Upsilon(11020)$  events in our data sample.  $\mathcal{B}$  is the number of background events in the signal region in the generic MC sample with the c.m. energy shifted to 11.022 GeV. We require  $M(K^+K^-)$  to be within  $m_\phi \pm 7.5(7.0) \text{ MeV}/c^2$  for category one (two), where  $m_\phi$  is the nominal mass of  $\phi$  [22]. The  $\phi$  mass sideband region is defined as  $M(K^+K^-) \in [1.000, 1.005]$  or  $[1.035, 1.040] \text{ GeV}/c^2$ . There is no evidence for the  $\chi_{bJ}$  signal in the  $\phi$  mass sideband events, nor in the generic MC sample (significance is less than  $0.1\sigma$  from the fit) mentioned above.

After applying all the selection criteria, the recoil mass spectra of  $\phi$  as a function of the initial beam four momenta from both data categories are shown in Fig. 3 for the sum of data in the energy region  $\sqrt{s} = 10.96\text{--}11.05 \text{ GeV}$ . We perform a simultaneous unbinned maximum likelihood fit to the  $\phi$  recoil mass spectra with the signal shapes from the simulated signal MC shapes, and a background shape obtained from data with the following procedure: a series of shapes are obtained from  $\Upsilon(5S)$  data, where, in calculating the  $\phi$  recoil mass, the c.m. energy is changed to that of each

individual data point, and summing up the shapes according to the luminosity. The ratios of the numbers of  $\chi_{b1}$  or  $\chi_{b2}$  events in the two categories are fixed according to the expected branching fractions of  $\chi_{b1}$  or  $\chi_{b2} \rightarrow \gamma\Upsilon(1S)$  [22] and the efficiencies. The fit results, which yield  $\chi^2/\text{ndf} = 104.2/55 = 1.9$ , are shown in Fig. 3. According to the fit,  $(1.5 \pm 0.5) \times 10^3 \chi_{b1}$  and  $(2.4 \pm 0.5) \times 10^3 \chi_{b2}$  events are produced. The statistical significances are found to be  $3.3\sigma$  and  $4.8\sigma$  for  $\chi_{b1}$  and  $\chi_{b2}$ , respectively.

When we vary the background shape by multiplying the nominal background shape with a first-, second-, or third-order polynomial, the smallest significances of the  $\chi_{b1}$  and  $\chi_{b2}$  signals are found to be  $2.6\sigma$  and  $2.1\sigma$ , respectively (multiplying by the third-order polynomial), yielding  $\chi^2/\text{ndf} = 43.6/49 = 0.89$ . The most conservative upper limits on the numbers of produced signal events in all the above tests are reported. After considering the systematic uncertainty which we discuss later, the upper limits for the produced numbers of  $\phi\chi_{b1}$  and  $\phi\chi_{b2}$  signal events are determined to be  $2.2 \times 10^3$  and  $3.1 \times 10^3$  at 90% confidence level (C.L.), respectively. The upper limits on the Born cross sections of  $e^+e^- \rightarrow \phi\chi_{b1}$  and  $\phi\chi_{b2}$  are 0.7 and 1.0 pb, respectively, averaged over the  $\Upsilon(11020)$  region, specifically  $\sqrt{s} = 10.96\text{--}11.05 \text{ GeV}$ . The calculation is based on Eq. (1), where the reconstruction efficiency, ISR correction factor, and vacuum polarization factor are averaged with weights according to the luminosity of each sample.

The sources of systematic uncertainties in the  $\phi\chi_{bJ}$  cross section measurement are similar to those of the  $\pi^+\pi^-\pi^0\chi_{bJ}$  modes, including the tracking efficiency, PID, photon detection, luminosity, trigger simulation, ISR correction,  $\phi$  mass window, and intermediate branching fraction. Most of these have been discussed in the  $\pi^+\pi^-\pi^0\chi_{bJ}$  analysis. The uncertainty from the  $\phi$  mass window requirement is found to be negligible by studying the consistency of the  $K^+K^-$  invariant mass between data and MC simulation. The uncertainty from the branching fraction of  $\phi \rightarrow K^+K^-$  is 1.0% [22]. The total systematic uncertainty for the cross section measurement is thus, combining all uncertainties in quadrature, 5.5% for either  $e^+e^- \rightarrow \phi\chi_{b1}$  or  $\phi\chi_{b2}$ .

In summary, using the energy scan data in the vicinity of the  $\Upsilon(11020)$  resonance, we observe the  $e^+e^- \rightarrow (\pi^+\pi^-\pi^0)_{\text{non-}\omega}\chi_{b1}$  process with significance of  $5.3\sigma$ . Evidence for  $\omega\chi_{bJ}$  is found but we cannot tell whether it is  $\omega\chi_{b1}$  or  $\omega\chi_{b2}$ . The limited statistics prevents us from drawing a conclusion concerning the origin of the signal events, that is, whether they arise from bottomonium decay, continuum production, or both. Since no continuum production of a multi-body final state with a bottomonium is known, it is natural to assume that the origin of the signal is bottomonium. Under this assumption, the branching fractions are  $\mathcal{B}(\Upsilon(10860) \rightarrow \pi^+\pi^-\pi^0\chi_{bJ}) = (2.5 \pm 0.6 \pm 2.1 \pm 0.7) \times 10^{-3}$ , which is compatible with the previous measurement [4], and  $\mathcal{B}(\Upsilon(11020) \rightarrow \pi^+\pi^-\pi^0\chi_{bJ}) = (8.7 \pm 4.3 \pm 6.1^{+4.5}_{-2.5}) \times 10^{-3}$ ,

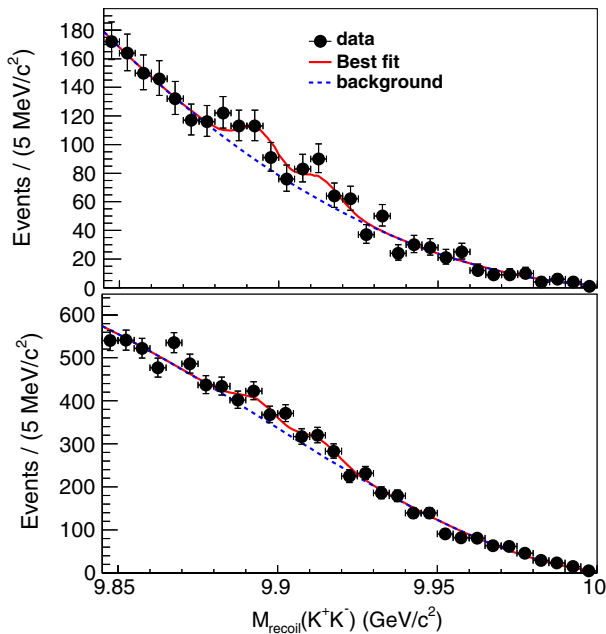


FIG. 3. The simultaneous fit results for data having  $M_{\text{recoil}}(\gamma K^+K^-)$ , with the recoiling mass of  $\gamma K^+K^-$ , in the  $\Upsilon(1S)$  mass window (up) and out of the  $\Upsilon(1S)$  mass window (down). Dots with error bars are data, the red solid lines are the best fit, and blue dashed lines are backgrounds.



which is compatible with the theoretical predictions [16]. Based on the 2D fit with summed data, the relative magnitude  $R_{21}(\omega) \equiv \frac{\mathcal{B}(\Upsilon(11020) \rightarrow \omega \chi_{b2})}{\mathcal{B}(\Upsilon(11020) \rightarrow \omega \chi_{b1})}$  can be estimated to be  $0.4 \pm 0.2$ , where the common systematic uncertainties cancel.

The processes  $e^+e^- \rightarrow \phi \chi_{bJ}$  are also searched for in data within  $\sqrt{s} = 10.96\text{--}11.05$  GeV, with no significant signals being observed. We report upper limits on the Born cross sections of  $e^+e^- \rightarrow \phi \chi_{b1}$  and  $\phi \chi_{b2}$  as 0.7 and 1.0 pb at 90% C.L., respectively. Compared with the total cross section of  $e^+e^- \rightarrow \Upsilon(11020)$ , these upper limits correspond to  $\Upsilon(11020)$  decay branching fractions of order  $10^{-3}$ , well above the theoretical predictions of order  $10^{-6}$  [16].

Our measurement of the transition rate agrees with the expectation of Ref. [16], but the measured relative magnitudes  $R_{21}(\omega)$  are significantly less than the theoretical predictions, which should be more reliable than the branching fraction predictions. This may inspire theorists to further investigate the discrepancy between the experimental measurement and the theoretical calculation.

## ACKNOWLEDGMENTS

We thank Dr. K. Li for his fantastic idea and kind help. We thank the KEKB group for excellent operation of the accelerator; the KEK cryogenics group for efficient solenoid operations; and the KEK computer group, the NII, and PNNL/EMSL for valuable computing and SINET5 network support. We acknowledge support from MEXT, JSPS and Nagoya's TLPSC (Japan); ARC (Australia); FWF (Austria); NSFC and the CAS Center for Excellence in Particle Physics (China); MSMT (Czechia); the Carl Zeiss Foundation (CZF), DFG, EXC153, and VS (Germany); DST (India); INFN (Italy); MOE, MSIP, NRF, Radiation Science Research Institute (RSRI), Foreign Large-size Research Facility Application Supporting project (FLRFAS), GSDC of KISTI and KREONET/GLORIAD (Korea); MNiSW and NCN (Poland); Ministry of Science and High Education and Russian Science Foundation (MSHE and RSF), Grant No. 18-12-00226 (Russia); ARRS (Slovenia); IKERBASQUE and MINECO (Spain); SNSF (Switzerland); MOE and MOST (Taiwan); and DOE and NSF (USA).

- 
- [1] Y.P. Kuang, QCD multipole expansion and hadronic transitions in heavy quarkonium systems, *Front. Phys. China* **1**, 19 (2006).
  - [2] K.F. Chen *et al.* (Belle Collaboration), Observation of Anomalous  $\Upsilon(1S)\pi^+\pi^-$  and  $\Upsilon(2S)\pi^+\pi^-$  Production Near the  $\Upsilon(5S)$  Resonance, *Phys. Rev. Lett.* **100**, 112001 (2008).
  - [3] I. Adachi *et al.* (Belle Collaboration), First Observation of the  $P$ -Wave Spin-Singlet Bottomonium States  $h_b(1P)$  and  $h_b(2P)$ , *Phys. Rev. Lett.* **108**, 032001 (2012).
  - [4] X.H. He *et al.* (Belle Collaboration), Observation of  $e^+e^- \rightarrow \pi^+\pi^-\pi^0\chi_{bJ}$  and Search for  $X_b \rightarrow \omega\Upsilon(1S)$  at  $\sqrt{s} = 10.867$  GeV, *Phys. Rev. Lett.* **113**, 142001 (2014).
  - [5] A. Bondar *et al.* (Belle Collaboration), Observation of Two Charged Bottomonium-Like Resonances in  $\Upsilon(5S)$  Decays, *Phys. Rev. Lett.* **108**, 122001 (2012).
  - [6] P. Krokovny *et al.* (Belle Collaboration), First observation of the  $Z_b^0(10610)$  in a Dalitz analysis of  $\Upsilon(10860) \rightarrow \Upsilon(nS)\pi^0\pi^0$ , *Phys. Rev. D* **88**, 052016 (2013).
  - [7] A. Garmash *et al.* (Belle Collaboration), Amplitude analysis of  $e^+e^- \rightarrow \Upsilon(nS)\pi^+\pi^-$  at  $\sqrt{s} = 10.865$  GeV, *Phys. Rev. D* **91**, 072003 (2015).
  - [8] K.-F. Chen *et al.* (Belle Collaboration), Observation of an enhancement in  $e^+e^- \rightarrow \Upsilon(1S)\pi^+\pi^-$ ,  $\Upsilon(2S)\pi^+\pi^-$ , and  $\Upsilon(3S)\pi^+\pi^-$  production around  $\sqrt{s} = 10.89$  GeV at Belle, *Phys. Rev. D* **82**, 091106 (2010).
  - [9] A. Abdesselam *et al.* (Belle Collaboration), Energy Scan of the  $e^+e^- \rightarrow h_b(nP)\pi^+\pi^-$  ( $n = 1, 2$ ) Cross Sections and Evidence for  $\Upsilon(11020)$  Decays into Charged Bottomonium-Like States, *Phys. Rev. Lett.* **117**, 142001 (2016).
  - [10] A. Ali, C. Hambrock, and M.J. Aslam, A Tetraquark Interpretation of the BELLE Data on the Anomalous  $\Upsilon(1S)\pi^+\pi^-$  and  $\Upsilon(2S)\pi^+\pi^-$  Production Near the  $\Upsilon(5S)$  Resonance, *Phys. Rev. Lett.* **104**, 162001 (2010); Erratum, *Phys. Rev. Lett.* **107**, 049903(E) (2011).
  - [11] N. Brambilla *et al.*, QCD and strongly coupled gauge theories: Challenges and perspectives, *Eur. Phys. J. C* **74**, 2981 (2014).
  - [12] M.B. Voloshin, Heavy quark spin symmetry breaking in near-threshold  $J^{PC} = 1^{--}$  quarkonium-like resonances, *Phys. Rev. D* **85**, 034024 (2012).
  - [13] F.K. Guo, U.G. Meissner, and C.P. Shen, Enhanced breaking of heavy quark spin symmetry, *Phys. Lett. B* **738**, 172 (2014).
  - [14] X. Li and M.B. Voloshin, Contribution of  $Z_b$  resonances to  $\Upsilon(5S) \rightarrow \pi\pi\pi\chi_b$ , *Phys. Rev. D* **90**, 014036 (2014).
  - [15] D.Y. Chen, X. Liu, and T. Matsuki, Explaining the anomalous  $\Upsilon(5S) \rightarrow \chi_{bJ}\omega$  decays through the hadronic loop effect, *Phys. Rev. D* **90**, 034019 (2014).
  - [16] Q. Huang, B. Wang, X. Liu, D.Y. Chen, and T. Matsuki, Exploring the  $\Upsilon(6S) \rightarrow \chi_{bJ}\phi$  and  $\Upsilon(6S) \rightarrow \chi_{bJ}\omega$  hidden-bottom hadronic transitions, *Eur. Phys. J. C* **77**, 165 (2017).
  - [17] D. Santel *et al.* (Belle Collaboration), Measurements of the  $\Upsilon(10860)$  and  $\Upsilon(11020)$  resonances via  $\sigma(e^+e^- \rightarrow \Upsilon(nS)\pi^+\pi^-)$ , *Phys. Rev. D* **93**, 011101 (2016).
  - [18] S. Kurokawa and E. Kikutani, Overview of the KEKB accelerators, *Nucl. Instrum. Methods Phys. Res., Sect. A* **499**, 1 (2003).
  - [19] A. Abashian *et al.*, The Belle detector, *Nucl. Instrum. Methods Phys. Res., Sect. A* **479**, 117 (2002).

- [20] D. J. Lange, The EvtGen particle decay simulation package, *Nucl. Instrum. Methods Phys. Res., Sect. A* **462**, 152 (2001).
- [21] R. Brun *et al.*, GEANT 3.21, CERN Report No. DD/EE/84-1, 1984.
- [22] C. Patrignani *et al.* (Particle Data Group), Review of particle physics, *Chin. Phys. C* **40**, 100001 (2016).
- [23] M. Benayoun, S. I. Eidelman, V. N. Ivanchenko, and Z. K. Silagadze, Spectroscopy at B factories using hard photon emission, *Mod. Phys. Lett. A* **14**, 2605 (1999).
- [24] E. Nakano, Belle PID, *Nucl. Instrum. Methods Phys. Res., Sect. A* **494**, 402 (2002).
- [25] S. S. Wilks, The large-sample distribution of the likelihood ratio for testing composite hypotheses, *Ann. Math. Stat.* **9**, 60 (1938).
- [26] S. Actis *et al.* (Working Group on Radiative Corrections and Monte Carlo Generators for Low Energies), Quest for precision in hadronic cross sections at low energy: Monte Carlo tools vs. experimental data, *Eur. Phys. J. C* **66**, 585 (2010).